ANALYSIS OF THE SOLAR POTENTIAL OF ROOFS
BY USING OFFICIAL LIDAR DATA

R. Kassner [a, *], W. Koppe [b], T. Schüttenberg [b], G. Bareth [b]

[a]solarkarte.com, Cologne, Germany - info@solarkarte.com
[b]GIS & Remote Sensing Group, Department of Geography, University of Cologne, Germany - g.bareth@uni-koeln.de

Commission IV, WgS IV/3

KEY WORDS: Image Processing, DSM, DEM, LIDAR, Texture Analysis, Feature Detection, Image Understanding, Geography

ABSTRACT:

This paper focuses on a field test that locates roof areas with a high solar potential and predicts the solar "harvest" per m^2. The test analyzes 2.5D LIDAR data provided by official surveying and mapping sources. The primary LIDAR data is prepared by masking the roofs' contours and afterwards filtering the point cloud by a threshold value. The remaining LIDAR data, which represents the buildings' roofs, is analyzed according to the slope, the azimuthal exposition and shaded roof areas. The quality assessment of the derived roof areas is carried out by means of a 3D dataset which is semiautomatically acquired from panchromatic stereophotogrammetric aerial photographs.

1. INTRODUCTION

Both a common awareness of the need to reduce CO_2 emissions and the rapidly rising energy costs have induced a growing demand for sustainable energies. Roof-mounted solar heating and photovoltaic systems are not only important technologies to decrease the emissions of carbon dioxide caused by domestic fuel consumption, but they also help saving energy and financial costs. Therefore, today the worldwide use of solar systems is increasing. Private investors as well as local authorities have a rising interest in identifying roof areas which are suitable for mounting solar systems.

Commonly LIDAR data is used to generate digital elevation models (DEM) (Kraus & Pfeifer, 1998; Kraus, 2001). Filtering and segmenting the LIDAR data leads to the recognition and the modeling of single objects, such as e.g. building extraction and reconstruction, and, on a larger scale, to 3D city modeling (Brenner, 2005; Ackermann, 1999; Chilton et al, 1999). As a consequence this technology and knowledge is also used for the analysis of solar potentials of roofs (Vögtle et al, 2005a; Vögtle & Tóvári, 2005b; Klärle & Ludwig, 2005).

Nowadays the cost of LIDAR data is comparatively low and the data is often provided by local authorities or state governments. An extensive automized use of airborne LIDAR data for locating roof areas suitable for mounting solar systems is to be expected in the near future.

2. TEST AREA & DATA SOURCES

2.1 Test Area

This field test is based on data referring to 13 buildings within the urban campus of the University of Cologne, Germany. The project was conducted in the framework of the CampusGIS-project where all required data for this study have been available. Due to its location on the fluvial planes of the river Rhine in the Cologne Bight, the morphoglogy of the campus area can generally be described as flat. These selected buildings comprise a variety of flat and sloped roofs, different complexities of the superstructure and different amounts of sections.

2.2 LIDAR data

For the analysis of the roofs, two primary irregular digital elevation models (DEM) of the campus area are used (Figure 1). The 2.5D point clouds of the digital terrain model (DTM) represent terrain surfaces at ground level, which means that vegetation and buildings are excluded. The digital surface model (DSM) provides height information on vegetation and buildings' surfaces. According to the specification given by the official surveying and mapping sources, the former "Landesvermessungsamt Nordrhein-Westfalen", the average point distance of the DTM is 1-5 m, whereas the distance of the DSM points is 1-2 m. The height accuracy is specified with +/- 50 cm for the DTM and +/- 30 cm for the DSM.
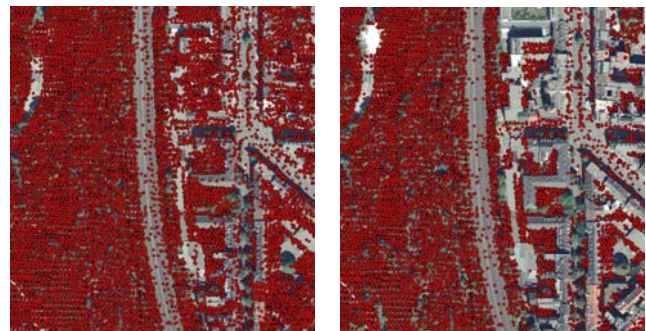

Figure 1. Irregular point clouds of the
LIDAR data (left: DSM; right: DTM)

2.3 Stereophotogrammetric Evaluation

The quality assessment of the results of the LIDAR data analysis is carried out by analyzing panchromatic

stereophotogrammetric aerial photographs of the test area. The pictures on the scale of 1:13.000 were also provided by the former "Landesvermessungsamt Nordrhein-Westfalen".

From the stereo pictures, a 3D model of each roof is created by using a Planicomp P33 analytical stereo plotter with an integrated CAD-interface (Figure 2). Once imported into a GIS environment, the CAD-models are rasterized and can afterwards be processed in the same way as the LIDAR dataset. Then it is possible to evaluate the quality of the results derived from the LIDAR data, namely their position, size, resolution and the percentage of correctly and falsely identified roof areas.
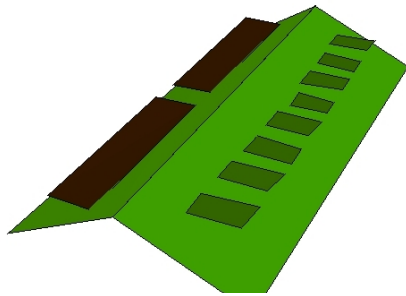

Figure 2. 3D CAD visualisation of the digitized stereophotogrammetric data for the purpose of evaluation

3. LIDAR DATA PREPARATION

3.1 Masking the Roof Areas

The LIDAR data is masked by the outlines of the buildings in order to obtain – by way of exclusion - those points that carry information about the elevation of the buildings' roofs. The outlines are derived from the 3D dataset which was generated for the purpose of the evaluation of the results. The roofs' outlines are imported to GIS and then converted to 2D layers. Other authors recommend the use of polygons originating from official cadastral databases (Vögtle & Tóvári, 2005b; Brenner & Haala, 1999) which usually are the only available datasource. Compared to official cadastral data, the outlines which are used for this approach have two advantages: Firstly, they represent the real shape and size of the roof, and not the dimension of the basement. And secondly, applying the same data as used for the evaluation ensures the comparability of the results during the process of the evaluation.

3.2 Filtering Incorrectly Positioned Points

The LIDAR points within the roofs' outlines still contain incorrectly positioned points representing the ground level height. They need to be eliminated according to their height. This is done in a way similar to that described by Haala (2005).

First the DTM pointcloud is rasterinterpolated, which leads to an extensive height information of the buildings' ground surface. Then all points within the roofs' outlines are filtered by introducing a threshold value of 3 m above the interpolated surface height (Figure 3). Now the remaining DSM points within the outlines can be used for the analysis of the solar potential of each roof.
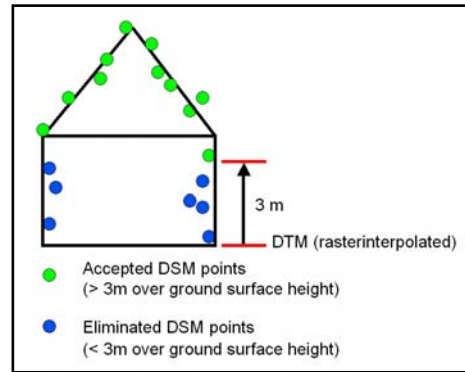

Figure 3. Threshold value filtering

4. ROOF ANALYSIS

4.1 Rooftype Identification

A raster interpolation of the remaining points leads to the classification of flat (<10°) and sloped (10°- 60°) roof areas, which, according to the prevailing percentage of classified area, allows a distinction of flat and sloped roofs.

Modeling flat roofs is comparatively easy as there is no need to deal with inclination (0°) or azimuthal exposition (e.g. 180° South). However, flat roofs need to be segmented in roof parts at different height levels. For this purpose it is necessary to classify the pointclouds of flat roofs. A distance of half the standard deviation between the classes is suitable. Then the points within each class can be filtered again to make sure that each roof patch is flat. This is also necessary to eliminate disturbing points that e.g. represent a tree towering above the roof.

4.2 Segmentation According to Slope and Inclination

In order to identify roof areas which are suitable for mounting solar systems, a combined assessment of the inclination and exposition of sloped roof buildings is necessary. A roof inclination between 10° and 60° is accepted as well as an azimuthal exposition between 90° East and 270° West. The identification of such areas is carried out by applying the GIS features "slope" and "aspect" on the rasterized dataset of each sloped roof. Those roof parts that fulfill both requirements can now be aggregated.

4.3 Roofshade Mmodeling

The GIS "hillshade" analysis function is used for the modeling of the shading of the different roof parts. By overlaying the shades, projected for different positions of the sun resulting from its daily and annual path along the celestial sphere, it is possible to identify shaded areas. Some 3D GIS applications as well as software tools, especially those designed for architects and engineers, offer the possibility for automatically calculating the shading. However, it has to be considered that the sun positions, which have to be chosen for modeling the shading, can depend on the respective set of preferences, like rentability, total amount of solar harvest or the total amount of available space to mount solar systems. Sloped roof elements e.g. will inevitably be shaded at certain daytimes, which does not necessarily mean that these areas cannot be used for collecting

solar energy. 3D modeling of the aggregated yearly amount of solar energy for each point on the roof is a promising way to get precise results.

4.4 Calculating the Solar Potential

Once the amount of square meters on a roof which are suitable for solar exploitation is known, a prognosis on the solar harvest of a building can be made. For Cologne, a solar harvest of ca. 400 kwh/m² per year for solar thermal collectors and ca 100 kwh/m² per year for photovoltaic modules can be simulated. The results have to be modified by a factor (Peuser et al, 2001) resulting from the derived information on slope and aspect of each roof segment.

5. RESULTS & DISCUSSION

The results of this field test make it clear that simple roof structures and high measure point densities generally lead to precise results. For the LIDAR data used in this study, after the filtering, there remains an average density of 1 measure point per 3 m² on an orthogonal projected surface. An average point density of 1 point per 4 m² results for sloped roof patches, which means that most of the small roof elements, e.g. dormers, cannot be identified.

Figure 4 shows that the classification according to the exposition of the different roof patches can lead to good results, even for more complex superstructures, if LIDAR data with a sufficient point density can be obtained. This roof for example is represented by 1 LIDAR measure point per 3m². However, it can also be seen that the roof patch at the building's southern end cannot be detected as there were no measure points available for this particular area.

In Figure 4 – 7, the yellow roof outlines are not identical with the contours in the corresponding ortho images because the aerial imagery is not orthorectified.
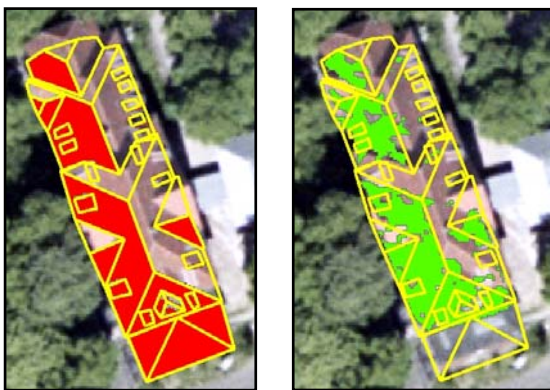

Figure 4. Segmentation of roof areas with an azimuthal exposition between 90° and 270° (left: evaluation data; right: LIDAR data)

The main problems that have to be considered when modeling LIDAR data on such a large scale are the limitations of the resolution of the DEM measure points and a possible inaccuracy of the points' position.
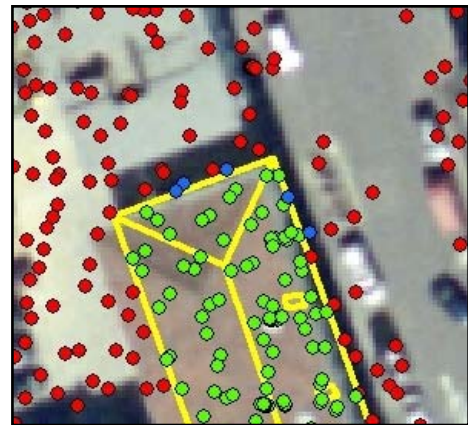

Figure 5. DSM measure points representing the roof´s height level which are eliminated by masking as they are positioned outside the building`s outline (blue points)

Figure 6. DSM measure points that represent the ground surface height inside the roof`s outline are eliminated by a 3m threshold value (blue points)

Inside and outside of the buildings' outlines an approx. 1.5 m wide band can be detected where displaced points are located. Figure 5 shows displaced measure points (blue points) that represent the roof's surface height. But as they lie outside the roof's outline they are eliminated by the masking. Figure 6 illustrates the same inaccuracy of the data inside the roofs' outlines. The blue measure points are actually at ground surface height or at a particular height level of the building's vertical facade, where the laserbeam incidentally hit the building's wall. They are eliminated by a 3 m threshold value segmentation. Brenner & Haala (1999) also confirm this problem of misplaced points in their contributions to 3D city modeling.

Misplaced DSM points do not only affect the modeling of the buildings' outer borders. They also cause problems as they impede a precise delimitation of different inner roof segments. This especially affects the modeling of different flat roof

elements at different heights along the edges of each flat roof segment. Problems resulting from misplaced points will be reduced by the use of next-generation LIDAR scanners with a higher resolution and precision. Furthermore, new algorithms and new 3D software will help to automatize the segmentation of roof elements and the removal of single points that differ from the general trend of each segment. Sitthole & Vosselman (2003) point out that a continuous improvement of the reliability of filtering is to be expected. However there will always remain ambiguities that cause problems when the data is processed (Nardinocchi et al, 2003).

Generally, areas along roof borders and also roof ridges cause problems. For example, calculating the slope leads to undesired flat areas here as can be seen in Figure 7. Height information makes measure points that are at a similar absolute height and are positioned on the opposite sides of the roof ridges fuse together and this falsely leads to the identification of flat areas. The same happens to the areas along the roof borders as there is no delimiting height information outside the buildings' outlines. The extent of those wrongly identified areas is interrelated with the point density of the supplied LIDAR data. The more points are available for an interpolation, the smaller will be the areas that are misinterpreted, especially at roof ridges.

Figure 7. Along roof borders and roof ridges areas can mistakenly be identified as flat (red patches)

The modeling of the roof shadows generally leads to good results. Most of the shaded areas on flat roofs are correctly modeled, as can be seen in Figure 8. The frayed look of the LIDAR model here is again due to a lack of resolution, not to the processing of the data. The results of the shade modeling for sloped roofs are not satisfying according to this field test. Again, the reason are the low resolution and the inaccuracy of the height information of the LIDAR data. Projecting shadows on distorted sloped roofs particularly leads to incorrect results because the inaccuracies of the roof models multiply due to the projection in the third dimension. However, these problems will also be solved as soon as better LIDAR scanner technology is in use.

is no easy way of distinguishing treetops from a roof's superstructure, if LIDAR data is used. This affects the segmentation of roofparts with overlapping treetops and leads to artefacts appearing in the roof models. On the other hand stereophotogrammetric digitizing methods are able to correct the data coverage by amodal completion of hidden roof parts and the generation of simplified tree models as well. To get correct results, trees need to be identified as such, their shape has to be remodeled with high resolution data and afterwards their shadows can be calculated. For processing aerial LIDAR

data, Matikainen et al (2007) have proposed new approaches to distinguishing between different objects. The combined analysis of LIDAR data and additional datasets, e.g. aerial colour ortho images or satellite imagery representing visible light and/or NIR, is promising. Analyzing shape patterns as well as spectral analysis can lead to the automized elimination of points in areas with an indicated vegetation.

Figure 8. Modeling the shadow with the evaluation data (left) and LIDAR data (right)

This field test demonstrates that the solar potentials of buildings' roofs can be calculated by the use of LIDAR data. Technically, the modeling of the azimuthal exposition, the slope and the shading can be carried out perfectly if the data sources are of sufficient quality. The quality improvement of the data is closely related to new filtering algorithms and techniques which improve the preprocessing of LIDAR data. In the future "ready to use" 3D city models will help to automatize the segmentation of roofs and other objects for modeling urban solar potentials. This will enable local authorities to provide exhaustive information about solar potentials within a foreseeable period. Even the price per solar factsheet for each building should be within the limits of usual official charges or even be offered for free.

REFERENCES

Ackermann, F., 1999. Airborne laser scanning – present status and future expectations. In: *ISPRS Journal of Photogrammetry and Remote Sensing*, 54(2&3), pp. 64-67.

Brenner, C., 2005. Building reconstruction from images and laser scanning. In: *International Journal of Applied Earth Observation and Geoinformation*, 6(3-4), pp. 187–198.

Brenner, C. & Haala, N., 1999. Towards Virtual Maps: On the Production of 3D City Models. *GeoInformatics*, 5(2), pp. 10-13.

Chilton, T.D., Jaafar, J. & Priestnall, G., 1999. The use of laser scanner data for the extraction of building roof detail using standard elevation derived parameters. In: *International Archives of Photogrammetry and Remote sensing*, La Jolla, USA, Vol. XXXII, Part 3, pp. 137-143.

Haala, N., 2005. Laserscanning zur dreidimensionalen Erfassung von Stadtgebieten. In: *3D-Geoinformationssysteme*, Heidelberg, Germany, pp. 26-38.

Klärle, M. & Ludwig, D., 2005. Standortanalyse für Photovoltaikanlagen durch hochauflösende Sensoren in der

Fernerkundung – Forschungsprojekt an der Fachhochschule Osnabrück. *GIS*, 6(4), pp. 16-18.

Kraus, K., & Pfeifer, N.; 1998. Determination of terrain models in wooded areas with airborne laser scanning data. In: *ISPRS Journal of Photogrammetry and Remote Sensing*, 53(4), pp. 193-203.

Kraus, K., 2001. Laser-Scanning - ein Pradigma-Wechsel in der Photogrammetrie. In: *21. Wissenschaftlich-Technische Jahrestagung der DGPF. Publikationen der Deutschen Gesellschaft für Photogrammetrie und Fernerkundung*, 10, Konstanz, Germany, pp. 13-22.

Matikainen, L., Kaartinen, H. & Hyyppä, J., 2007. Classification of tree based building detection from laser scanner and aerial image data. In: *The International Archives of the Photogrammetry, Remote Sensing and Spatial Information Sciences*, Espoo, Finland, Vol. XXXVI, Part 3, pp. 280-287.

Nardinocchi, C., Forlani, G. & Zingaretti, P., 2003. Classification and filtering of laser data. In: *3-D reconstruction from airborne laser scanner and InSAR data - Proceedings of the ISPRS working group III/3 workshop*, Dresden, Germany, Vol. XXXIV, Part 3.

Peuser, F., Remmers, K.-H. & Schnauss, M., 2001. *Langzeiterfahrung Solarthermie*. Solarpraxis, Berlin, p. 350.

Sithole, G. & Vosselmann, G., 2003. Comparison of Filtering algorithms. In: *3-D reconstruction from airborne laser scanner and InSAR data - Proceedings of the ISPRS working group III/3 workshop*, Dresden, Germany, Vol. XXXIV, Part 3, pp. 71-78.

Vögtle, T., Steinle, E. & Tóvári, D., 2005a. Airborne Laserscanning Data for determination of suitable areas for photovoltaics. In: *International Archives of Photogrammetry and Remote Sensing*, Enschede, the Netherlands, Vol. XXXVI, Part 3, pp. 215-220.

Vögtle, T. & Tóvári, D., 2005b. Welches Dach eignet sich für Photovoltaik. In: *GeoBIT*, 17(12), pp. 23-25.